

Initial Helioseismic Observations by Hinode/SOT

Takashi SEKII¹, Alexander G. KOSOVICHEV², Junwei ZHAO², Saku TSUNETA¹, Hiromoto SHIBAHASHI³, Thomas E. BERGER⁷, Kiyoshi ICHIMOTO¹, Yukio KATSUKAWA¹, Bruce W. LITES⁴, Shin'ichi NAGATA⁵, Toshifumi SHIMIZU⁶, Richard A. SHINE⁷, Yoshinori SUEMATSU¹, Theodore D. TARBELL⁷, and Alan M. TITLE⁷

¹*National Astronomical Observatory of Japan, Mitaka, Tokyo 181-8588*

sekii@solar.mtk.nao.ac.jp

²*W. W. Hansen Experimental Physics Laboratory, Stanford University, Stanford, CA 94305, USA*

³*Department of Astronomy, School of Science, University of Tokyo, Bunkyo-ku, Tokyo 113-0033*

⁴*High Altitude Observatory, National Center for Atmospheric Research, P.O. Box 3000, Boulder, CO 80307, USA*

⁵*Kwasan and Hida Observatories, Kyoto University, Kuravashira, Kamitakara-cho, Takayama, Gifu, 506-1314*

⁶*Institute of Space and Astronautical Science, Japan Aerospace Exploration Agency, 3-1-1 Yoshinodai, Sagami-hara, Kanagawa 229-8510*

⁷*Lockheed Martin Solar and Astrophysics Laboratory, B/252, 3251 Hanover St., Palo Alto, CA 94304, U.S.A.*

(Received 2007 July 27; accepted)

Abstract

Results from initial helioseismic observations by Solar Optical Telescope onboard Hinode are reported. It has been demonstrated that intensity oscillation data from Broadband Filter Imager can be used for various helioseismic analyses. The $k - \omega$ power spectra, as well as corresponding time-distance cross-correlation function that promises high-resolution time-distance analysis below 6-Mm travelling distance, were obtained for G-band and Ca II-H data. Subsurface supergranular patterns have been observed from our first time-distance analysis. The results show that the solar oscillation spectrum is extended to much higher frequencies and wavenumbers, and the time-distance diagram is extended to much shorter travel distances and times than they were observed before, thus revealing great potential for high-resolution helioseismic observations from Hinode.

Key words: Sun: helioseismology — Sun: interior — Sun: oscillations

1. Introduction

Local helioseismology has been a great success in revealing subsurface structure of the sun, particularly in detecting three-dimensional flow and sound-speed anomaly in active regions (see, e.g., Zhao, Kosovichev & Duvall 2001, Zhao & Kosovichev 2003).

Observations for local helioseismology require high resolution and wide coverage both in space and in time. The 50-cm aperture Solar Optical Telescope (SOT, Tsuneta et al. 2007; Suematsu et al. 2007) onboard Hinode satellite (Kosugi et al. 2007) provides 0.2-arcsec spatial resolution though with a limited field of view (328 arcsec \times 164 arcsec for Narrowband Filter Imager (NFI) and 218 arcsec \times 109 arcsec for Broadband Filter Imager (BFI), nominally). Except during the satellite eclipse periods, Hinode can observe the sun continuously with cadence up to 15 s or even less, with the actual limit placed by telemetry bandwidth and capacity of the data recorder, which are shared with other instruments as well as other SOT programs running at the same time frame.

The high resolution of SOT particularly offers a great potential for local helioseismology. One of the main scientific targets of Hinode is to investigate the generation, evolution and eventual dissipation of active regions on the sun, in attempt to observationally constrain theories on dynamo processes which are thought to be responsible for

the solar activity cycle. Local helioseismology can contribute greatly in this area, not only via active region tomography but also in measuring flows at larger scales such as meridional flow, which plays an important role in the current models of solar activity cycle (Dikpati & Gilman 2006). Please note that even with the limited field of view of SOT, and hence the limited depth coverage for tomographic study (see below), one can still measure near-surface components of large-scale flows in a small area first but then extend the measurement to a broader area simply by repeating the observation at different locations.

It was planned to use Dopplergrams produced by NFI for helioseismic observations on Hinode (Sekii et al. 2001; Sekii 2004). Not only oscillation signals in Dopplergrams are known to exhibit higher signal-to-noise ratio than oscillation signal in intensity, but also NFI has a larger field of view than BFI. A larger field of view translates into a better depth coverage for tomography, because waves that penetrate deeper into the sun also travels further in horizontal directions. Thus NFI Doppler observation was the preferred mode of helioseismic observation by Hinode.

However, long series of Dopplergrams are still only being tested at the time of writing. Instead, we examined BFI intensity oscillation data from H line (Ca II) and G band (CH).

The main aim of the present paper is to report that helioseismic observations can indeed be made with BFI.

As an example, a result from our first attempt at time-distance analysis of subsurface flow is presented.

2. Data analysis

A quiet region around the disk center was observed from around 1600UT, 1 Jan 2007, to around 0400UT, 2 Jan 2007, for about 12 hours with a 12-minute interruption in the middle of the run. Hinode was tracking the region during the observation (except during the interruption mentioned in the above) and in addition Correlation Tracker was used to maximize frame-to-frame correlation in the central region of the field of view (Shimizu et al. 2007). No further tracking was done on ground, unlike in the case of a sunspot study (Nagashima et al. 2007).

Both G-band images and Ca II-H images were acquired at approximately 1-min cadence, Ca II-H images following G-band images by 20 s. Sample images are shown in figure 1. The CCD pixels were 2×2 summed onboard to reduce the data amount, to double the effective pixel size to 0.106 arcsec. We applied another 2×2 summing on ground (the overall result was a 4×4 summing) for the sake of faster analyses, though in this case we no longer fully exploit the 0.2-arcsec resolution of the telescope. The benefit of using the full 2×2 -summed data, or observing with the full capacity of SOT (no summing), will be investigated in future work.

The cadence was not exactly regular, due to the fact that there are two clocks involved in controlling the equipment. Not only they are on different cycles (0.5 s for Mission Data Processor and 1.6 s by Polarization Modulator Unit), the clocks are slowly drifting away from each other. Although programming tricks to correct this behavior are being investigated and tested, they have not been applied to the current datasets.

A simple test was run to check the effect of the slightly irregular cadence, by putting through a sine wave on this irregular temporal grid and then computing power spectrum, pretending that the cadence was exactly 1 minute. As we expected, the effect was insignificant and therefore we carried out all the following analyses assuming that the cadence was exactly 1 minute.

The projection effect was also neglected. Because the BFI field of view is so narrow it should not give rise to any significant inaccuracy around the disk center.

We used only the first uninterrupted 6-hr of the data for basic diagnostics products in the next section. For the time-distance analysis, the full 12-hr data were used. Before starting the analyses that follow, first we applied running difference of images: each image was subtracted from the following image, thus obviating the need for calibrating each image for dark, flat field and bad pixels. One might worry that employing the running difference might increase the noise level, if the cadence is too short compared to the time scale over which the signal changes, in which case the differences between two successive frames are dominated by noise. This is not the case here, when the 1-min cadence is not too high for the oscillation signal that is dominated by 5-min oscillations.

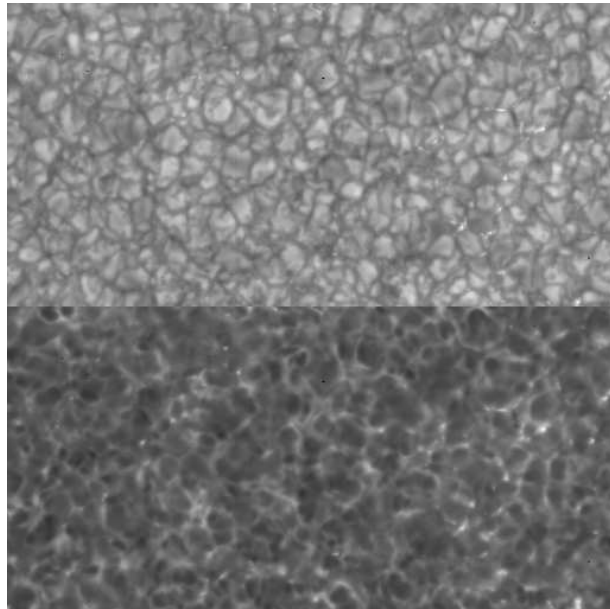


Fig. 1. Sample images of the observed region in G band (top) and Ca II H line (bottom). Of the full field of view which is $218 \text{ arcsec} \times 109 \text{ arcsec}$, only the central part of the left half (approximately $54 \text{ arcsec} \times 27 \text{ arcsec}$) is shown.

3. Power spectra and time-distance diagram

In this section we present the most basic products of helioseismic observations: the so-called k - ω diagram (or l - ν diagram) and the time-distance diagram. They are then compared with results obtained from Michelson Doppler Imager (MDI) onboard Solar and Heliospheric Observatory (Scherrer et al. 1995). The MDI data we used were acquired in the high-resolution mode. Although they too cover the central region of the disk, they are not coeval with the SOT data.

Figure 2 shows the k - ω diagrams obtained from G-band and Ca II-H data; the series of the differential intensity-field data (intensitygram) were Fourier transformed and converted to power spectra, which were then azimuthally integrated in wavenumber space. Although no spherical-harmonic decomposition was involved, degree l was assigned to each component by multiplying its wavenumber by the solar radius. The power spectra were corrected for the ω^2 factor, where ω is angular frequency, for we have taken running difference before Fourier transform.

In spite of only 6 hours of observation, the f-mode ridge is seen up to $l \approx 4000$. We also see the high-frequency interference peaks (Jefferies et al. 1988, Duvall et al. 1991, Kumar et al. 1990) up to the Nyquist frequency. They seem disturbed close to the Nyquist frequency because the ridges from both the super- and sub-Nyquist ranges are running into the other regime. Compared to the k - ω diagram obtained from a 512-min MDI high-resolution velocity dataset, also shown in figure 2, the better performance of SOT at high-wavenumber, where high-resolution matters most, is noticeable in how the f-mode ridge extends to higher wavenumbers and, in the case of Ca II H

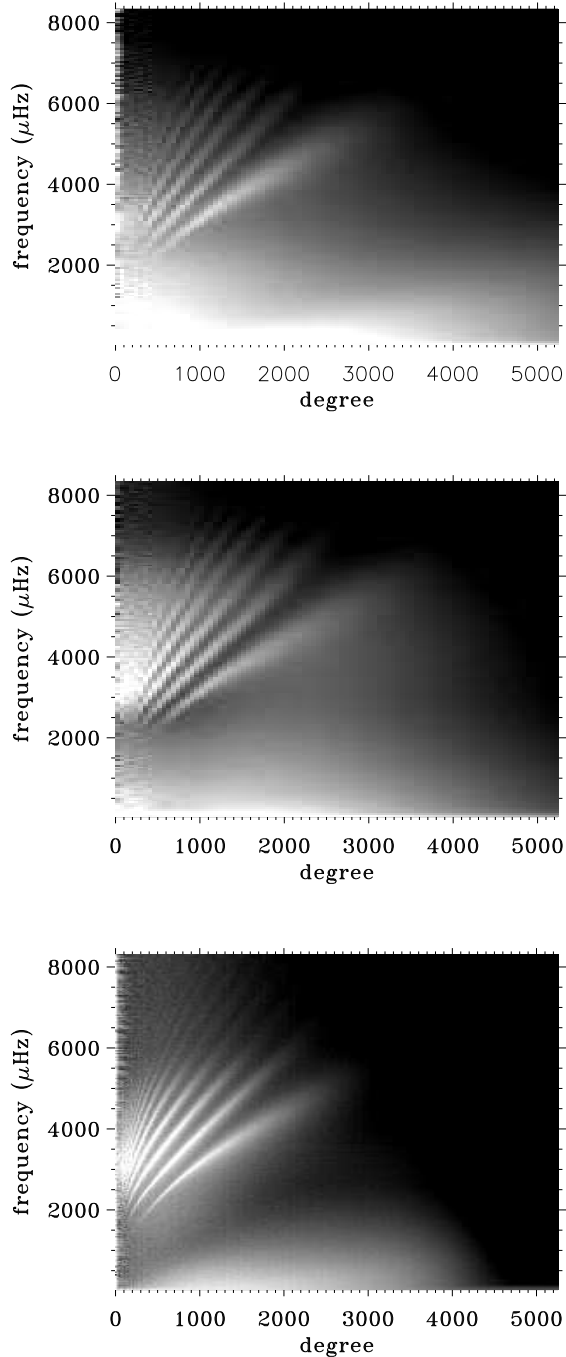


Fig. 2. Power spectra (k - ω diagrams) from the 6-hr G-band data (top) and Ca II-H data (middle), compared with power spectrum from a 512-min MDI high-resolution Doppler data (bottom).

data, the p_1 ridge as well. However, as was expected, the SOT k - ω diagrams show higher background-noise level compared to the Doppler measurement by MDI.

It is apparent that in G-band data the convective 'noise' is stronger and for this reason, in the following analyses, we use only Ca II H data. More detailed comparison between the two, in particular phase relations at various frequencies, would be a subject of future work.

We then applied Fourier-Bessel transform (see, e.g., Sekii & Shibahashi 2003) to the Ca II-H k - ω power spectrum to obtain time-distance cross-correlation function (figure 3). The power spectrum uncorrected for the ω^2 was used; this may be viewed as an application of a broad high-pass filter to the power spectrum, the intention being filtering out the convective noise.

The structure down to less than 0.1 heliographical degree is seen with a high signal-to-noise ratio, which is very encouraging. Once again, we see the higher performance of SOT, compared to MDI, also shown in figure 3, at small spatial scales. The signal-to-noise ratio, however, is higher for MDI at large distances and thus the both instruments complement each other.

4. Subsurface flow

We have analyzed the full 12-hr long series by time-distance technique for local helioseismology. The gap between the two 6-hr stretches was filled with zeroes. Then for measuring travel-time difference between outward and inward wave components, each pixel was cross-correlated with average signals over annuli that cover, in radii, 4.00-6.62, 6.47-9.70, 9.24-12.47, 12.01-15.86, 15.09-18.94, 18.48-22.33, and 21.56-25.41 (all in Mm). One such example as well as an MDI counterpart (in high-resolution mode) is shown in figure 4. The annuli were further divided into 4 sectors representing north, south, east and west, and opposing pairs of sectors were similarly cross-correlated to yield northward-southward and westward-eastward travel-time differences.

All the travel-time differences were then inverted by using ray-approximation kernel for acoustic wave propagating through the solar interior. Figure 4 shows outward-inward travel-time difference map, as a proxy divergence of the flow field. Inversions for horizontal flow in the depth ranges of 0-1 Mm, 1-2 Mm, 2-3 Mm and 3-4 Mm are shown in figure 5. Inversions were done for the entire area in figure 4, but to avoid overcrowding the figure with arrows, in figure 5 only the central quarter is shown. Horizontal flow patterns are largely consistent with the outward-inward travel-time difference, as was seen in realistic numerical simulation by Zhao et al. (2007). This indicates that the travel-time difference is a good proxy of flow divergence, though to acquire additional details we do need inversion procedure. We see that supergranulation patterns are coherent vertically within a spatial scale of a few Mm.

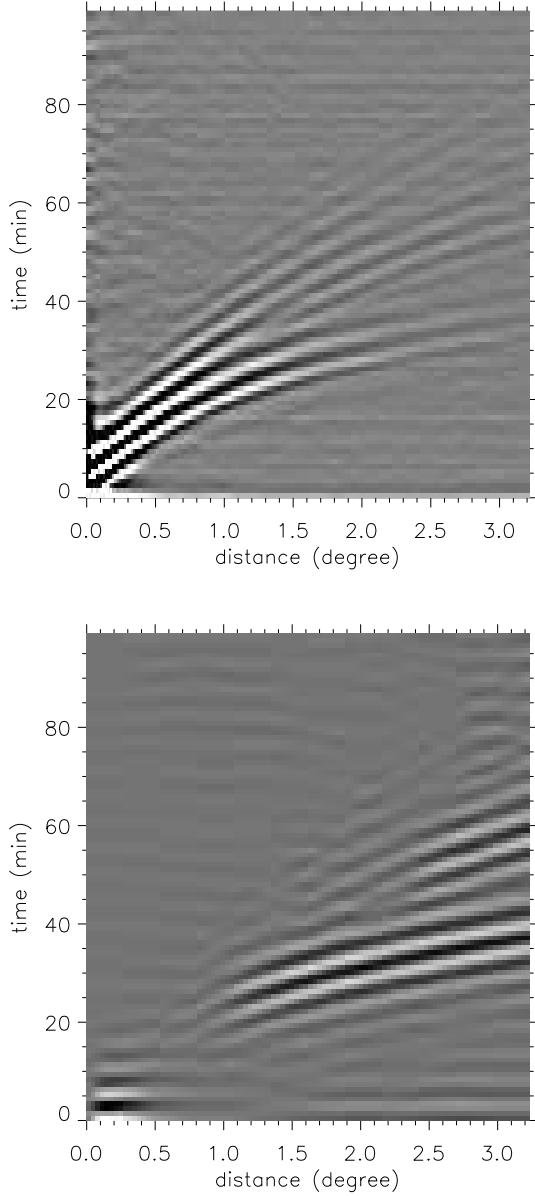


Fig. 3. Time-distance diagrams from 6-hr Ca II-H data (top) and from 512-min MDI high-resolution Doppler data (bottom). The datasets are not co-eval.

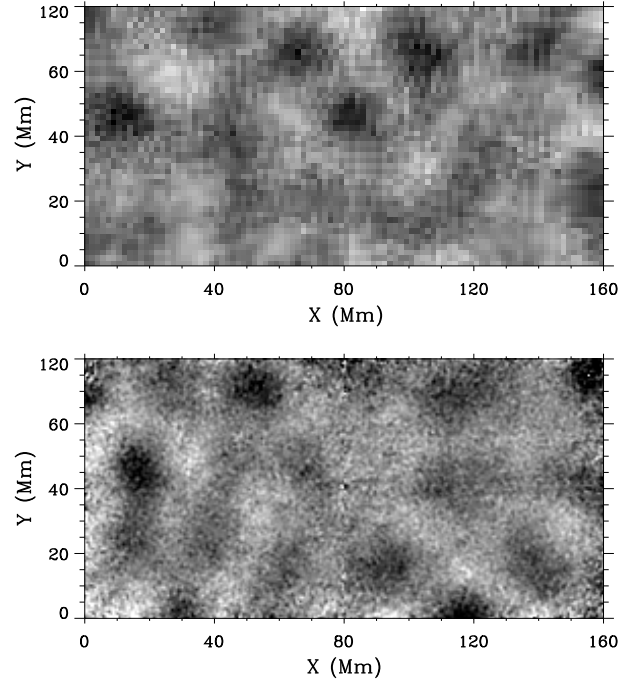


Fig. 4. An outward-inward travel time difference maps from 512-min MDI high-resolution Doppler data (top) and from Ca II-H data (bottom), indicating flow divergence due to supergranulation. The inner radius of the annulus used was 13.86 Mm and the outer radius 15.86 Mm. Dark patches are where inward travel time is longer than outward travel time i.e. where the flow is generally diverging, whereas brighter patches are where the flow is generally converging. Since the two datasets are not co-eval, individual features are not to be compared directly.

5. Discussion

As we have demonstrated, SOT observation of intensity oscillations can be used for high-resolution helioseismic diagnosis of the sun, in spite of its noise level higher than what can be expected from Doppler measurement. This is due to the fact that solar noise is higher in intensity than in Doppler velocity.

From figure 2 it is apparent that SOT offers good opportunity to study high-wavenumber waves, particularly f modes. Ishikawa et al. (2007) has found ubiquitous small-scale horizontal magnetic field from Hinode/SOT observation of the photosphere. In addition to turbulence, presence of such magnetic fluxes would affect propagation of f-mode waves and this would be an important future work.

In the time-distance cross-correlation (figure 3), the structure below 0.5 degree, which is about the distance of 6 Mm, has been observed much clearer than before. Sekii (2004) used G-band data obtained from 50-cm La Palma SVST to demonstrate somewhat similar enhancement in spatial resolution but the noise level was much higher. It was speculated that the noise came mainly from atmospheric seeing and that the spaceborne SOT would perform better. Our current results show that SOT indeed does. Figure 4 demonstrates that study of fine structures

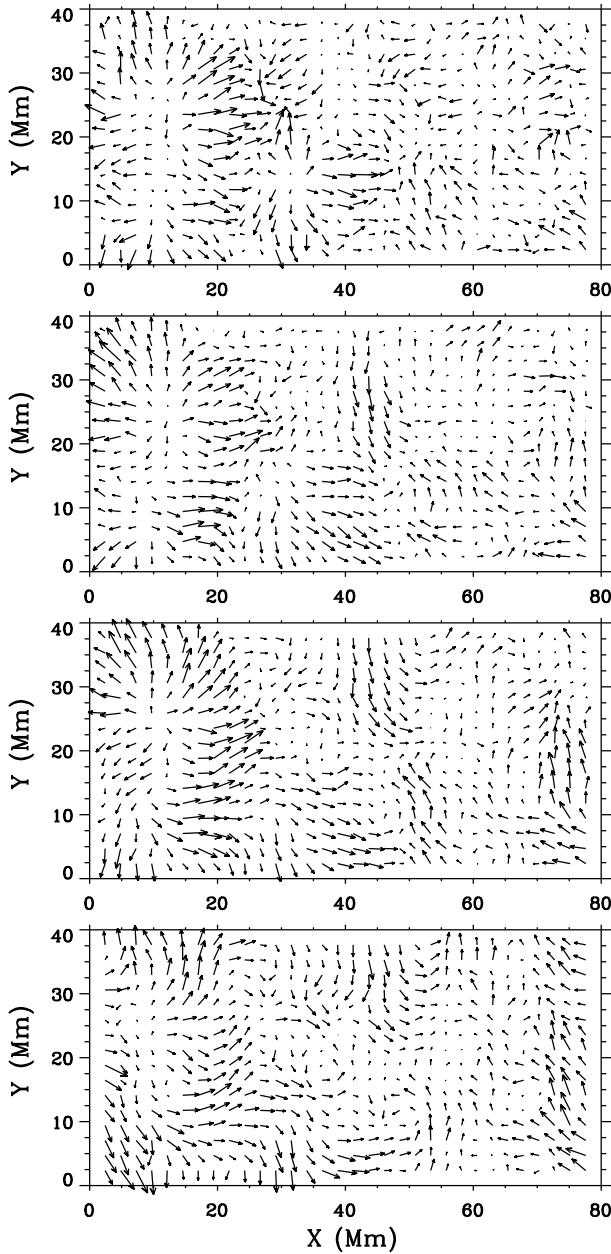


Fig. 5. Subsurface flow maps (indicated by arrows) obtained by time-distance analysis of 12-hr Ca II-H data. Depth ranges are 0 – 1 Mm, 1 – 2 Mm, 2 – 3 Mm and 3 – 4 Mm (top to bottom). The longest arrow in the panels correspond to 0.51 km s^{-1} , 0.52 km s^{-1} , 0.30 km s^{-1} and The field of view corresponds to the central quarter of the field of view in figure 4.

in supergranulation patterns benefits from the high resolution of SOT; the bright and dark patches have a typical spatial scale of 20 Mm but a transition from bright to dark takes place over the scale of less than 10 Mm, which MDI have difficulty in resolving. With SOT results we see smoother transitions.

To exploit this small-scale information would require more tuning and testing of the inversion, particularly the setup of annuli. The trade-off between resolution and error need to be examined carefully. Once done, we will certainly achieve higher horizontal resolution in time-distance inversions. A similar improvement in performance is expected in resolving, vertically, layers immediately below the surface, since SOT can use higher-wavenumber and hence shallower-penetrating waves. This applies also to sound-speed inversion, which has not been attempted yet.

Time-distance analysis in active regions, be it for flow or for thermal (and even magnetic) structure, would need further care particularly if we wish to go a step beyond phenomenological inversions; wave propagation in magnetized atmosphere has to be somehow taken into account. For the initial analysis of sunspot oscillation data, see Nagashima et al. (2007).

Hinode is a Japanese mission developed and launched by ISAS/JAXA, collaborating with NAOJ as a domestic partner, NASA and STFC (UK) as international partners. Scientific operation of the Hinode mission is conducted by the Hinode science team organized at ISAS/JAXA. This team mainly consists of scientists from institutes in the partner countries. Support for the post-launch operation is provided by JAXA and NAOJ (Japan), STFC (U.K.), NASA, ESA, and NSC (Norway). This work was carried out at the NAOJ Hinode Science Center, which is supported by the Grant-in-Aid for Creative Scientific Research “The Basic Study of Space Weather Prediction” from MEXT, Japan (Head Investigator: K. Shibata), generous donations from Sun Microsystems, and NAOJ internal funding.

References

- Dikpati, M., & Gilman, P. A. 2006, *ApJ*, 649, 498
- Duvall, T.L., Jr., Harvey, J.W., Jefferies, S.M., Pomerantz, M.A. 1991, *ApJ*, 373, 308
- Ishikawa, R., et al. 2007, submitted to *Science*.
- Jefferies, S.M., Pomerantz, M.A., Duvall, T.L., Jr., Harvey, J.W., Jaksha, D.B. 1988, in *Seismology of the Sun and Sun-like Stars*, ed. V. Domingo & E.J. Rolfe (Noordwijk, ESA Publication Division), 279
- Kosugi, T., et al. 2007, to be submitted to *Sol. Phys.*
- Kumar, P., Duvall, T.L., Jr., Harvey, J.W., Jefferies, S.M., Pomerantz, M.A., Thompson, M.J. 1990, in *Progress of Seismology of the Sun and Stars*, ed. Y. Osaki & H. Shibahashi (Springer-Verlag, Berlin), 87
- Nagashima, K. et al. 2007, submitted to *PASJ*
- Scherrer, P. H., et al. 1995, *Sol. Phys.* 192, 261
- Sekii, T. 2004, in *The Solar-B Mission and the Forefront of Solar Physics: The Fifth Solar-B Science Meeting*, ed. T. Sakurai & T. Sekii (San Francisco: ASP), 89

- Sekii, T., Shibahashi, H., Kosovichev, A. G., Duvall, T. L., Jr., Berger, T. E., Bush, R., & Scherrer, P. H. 2001, in SOHO 10/GONG 2000 Workshop: Helio- and Asteroseismology at the Dawn of the Millenium, ed. P. Pallé & A. Wilson (Noordwijk, ESA Publication Division), 327
- Sekii, T., & Shibahashi, H. 2003, in SOHO 12/GONG+ 2002: Local and Global Helioseismology: The Present and Future, ed. H. Sawaya-Lacoste (Noordwijk, ESA Publication Division), 389
- Shimizu, T., et al. 2007, submitted to Sol. Phys.
- Suematsu, T., et al. 2007, submitted to Sol. Phys.
- Tsuneta, S., et al. 2007, submitted to Sol. Phys.
- Zhao, J., Georgobiani, D., Kosovichev, A. G., Benson, D., Stein, R. F., & Nordlund, Å 2007, ApJ, 659, 848
- Zhao, J., & Kosovichev, A. G. 2003, ApJ, 591, 446
- Zhao, J., Kosovichev, A. G., & Duvall, T. L., Jr. 2001, ApJ, 557, 384.